PAPER • **OPEN ACCESS**

Impact and bending analysis of composite scarf adhesive joints modified with MWCNTs at room and hot temperatures

To cite this article: U A Khashaba *et al* 2019 *IOP Conf. Ser.: Mater. Sci. Eng.* **610** 012007

IOP Conf. Series: Materials Science and Engineering **610** (2019) 012007 doi:10.1088/1757-899X/610/1/012007

Impact and bending analysis of composite scarf adhesive joints modified with MWCNTs at room and hot temperatures

U A Khashaba[1,2,3], Ramzi Othman[1] and I M R Najjar[1]

[1] Mechanical Engineering Department, Faculty of Engineering, King Abdulaziz University, P.O. Box 80204, Jeddah 21589, Saudi Arabia
[2] Mechanical Design and Production Engineering Department, Faculty of Engineering, Zagazig University, Egypt

[3] Email: khashabu@zu.edu.eg

Abstract. Scarf adhesive joints (SAJs) have attracted an increasing attention in joining/repairing of carbon-fiber reinforced epoxy (CFRE) composite structures due to their zero eccentricity, which provides better aerodynamic surfaces. This study evaluated for the first time, the performance of SAJs in CFRE composites under thermo-mechanical impact loads. The adhesive was modified with optimum percentage of multi-walled carbon nanotubes (CNTs). The impact tests were performed at room temperature of +25°C, +50°C and +75°C. The residual flexural properties of the unfailed impacted joints were measured using three-point bending test. Results from impact tests at temperature of 25°C, 50°C and 75°C showed improvement in the impact bending stiffness of the modified SAJs with CNTs by 8.3%, 7.4% and 11.8% and maximum contact force by 15.6%, 21.3% and 18.9%, respectively. The energy at failure of the CNT-SAJs was increased by 15.2% and 16.4% respectively at temperatures of 25°C and 50°C. At test temperature of 75°C the SAJs have hysteresis load-displacement behavior and energy-time curve with rebound energy of 35% and absorbed (damage) energy of 65%. The residual flexural strength of the modified and unmodified SAJs is 98.2% and 86.1% respectively, while their residual moduli have remarkable decrease to 71.7% and 81.3%.

Keywords: Scarf adhesive joint, Multi-walled carbon nanotubes, Thermo-mechanical impact loads, Impact bending stiffness, Absorbed energy, Bending tests.

1. Introduction

Fiber-reinforced polymer (FRP) composites offer a number of distinct advantages compared to conventional engineering metallic materials, such as high specific strength and stiffness, excellent vibration damping capacity, superior corrosion and fatigue resistance. Accordingly, they have been extensively used as structural components in aircraft and space applications as well as for automotive parts. In these applications adhesive joining/repairing cannot be avoided for assembly and repair purposes of the structure components [1]. Scarf adhesive joints (SAJs) have attracted considerable attention because of their zero eccentricity along the load path and provide better aerodynamic surfaces [2] relative to other bonded joints. The demand for improving the performance of the SAJs in composite structures is required forever and is the subject of the current study.

The present paper is a continuation of previous work of Khashaba et al. [3-8], with the objective to obtain most of the mechanical properties of the SAJs in carbon fiber reinforced polymer (CFRP) composites modified with different nanofillers. Frist, the optimum weight percentage of the different nanofillers was determined experimentally [3] and used to fabricate SAJs with different scarf angles [4,5]. The SAJs were subjected to tensile loads at room temperature, hot and moist conditions [4,5]. The measured values of the ultimate tensile strength agreed well with that predicted using three-dimensional finite element analysis models. Fatigue analysis was studied through different relationships, which include S-N curves [6-8], stiffness-N curves and load-displacement hysteresis loops [7]. Statistical and reliability analysis were conducted on fatigue life data to estimate the safe fatigue life at different reliability levels [6,7].

Any selection of joint characteristics for optimal design should be based on trade-of between the different mechanical properties. During service life, the structural components were subjected to low-velocity impact loads, like tools drop during maintenance processes, hammer and tire debris impact. These low-velocity impact loads can induce degradation of the composite structure, which sometimes is hard to detect by visual inspection. Accordingly, the main objective of the present study is to investigate the performances of the SAJs modified with CNTs in CFRE composites under bending and thermo-mechanical impact loads, which are not investigated yet.

As there is no standard specification for testing the SAJs [9], care should be taken when describing the gain/loss in the mechanical properties relative to the scarf angle. Jen [10] defined the scarf angle as the angle between the plane normal to the joint axis and the bonding line. While the scarf angle in the present study and the other researchers cited in this paper, was defined as the angle between the plane parallel to the specimen axis and the bonding line.

At high temperature, the difference in the coefficients of thermal expansion of the reinforcing carbon fibers, CNTs and the adhesive material could be significant enough to cause microcracks initiation in the tapered adherends as well as interfacial shear failure before applying the impact loads. Nguyen et al. [11] studied the effect of test temperatures on the tensile properties of steel/CFRP adhesively-bonded double strap joints. They have reported that the joint failure mode changed from adherend failure to debonding failure as the temperature approached the glass transition temperature of the adhesive. In addition, the ultimate load and joint stiffness decreased by about 15%, 50% and 80% when temperatures increased by 0°C, 10°C, and 20°C above T_g, respectively. Through the literature review, the authors found that, the properties of the SAJs under thermo-mechanical impact loads has not yet been reported, which is the main reason that motivated the authors to perform this study.

Improving the impact properties of the scarf adhesive joints in composite structures via incorporation of CNTs into the adhesive material has not yet fully explored in the literature. However, there are a few available data on the performance of the scarf joints bonded with neat adhesives [12,13] and modified adhesives with micro-fillers [14,15] under mechanical impact loads. Kim et al. [12] studied the impact properties of the composite laminates and composite scarf repairs subjected to in-plane tensile loading. They have reported that pre-strain has a negligible effect on the delamination size in composite laminates for the given impact energy of 8 J. On the other hand, a mixed damage of adhesive disbonding and adherend delamination was observed and increases significantly with increasing pre-strain levels. Delamination in composite adherends has been found to reduce the size of adhesive disbonding. Sato and Ikegami [13] found that The SAJ is the most effective shape to minimize the stress concentration in the adhesive layer under static loading as well as under dynamic loading compared with tapered lap joints and single lap joints.

Ali et al. [14] found that incorporation of microparticles led to a significant improvement of the impact load bearing capacity of the scarf joints and reduced the extent of the damage area. Recently, Ozdemir and Oztoprak [15] reported improvements in impact resistance, at room temperature, of single-lap composite joints bonded by fiber-reinforced polymer. However, the tensile failure load of the modified joints decreases with the increasing test temperature from room temperature to 75°C.

Introducing of CNTs into the adhesive materials can play contrary roles in deciding the performance of composite bonded joints especially at higher temperatures near the glass transition

temperature. CNTs can improve the mechanical properties of the epoxy adhesive as a reinforced material as well as improving their glass transition temperature [16-19] and thus, delay their softening temperature as well as thermal fracture. However, T_g is not a material property and dependent CNTs (raw or functionalized), wt% of CNTs, the measurement technique and the experimental conditions used (e.g. heating rate, sample size). Gojny et al. [19] found improvement of 8°C in the T_g of the modified epoxy with same wt% of CNT (0.5 %) and dispersion processing technique (ultrasonic dispersion) of the present study. On the other hand, CNTs can improve the thermal conductivity of the adhesive layer, which can leads to rapid distribution of the temperature with more softening and thus, reducing the joint strength. The thermal conductivity of multi-walled CNTS is (= 3000W/mK[20,21]) very high compared with epoxy adhesive (0.3 W/mK[20]) and some famous metals such as Aluminum (= 210 W/m°C). Korayem et al. [16,17] reported that incorporation of 3.0 wt% CNTs into epoxy adhesive of CFRP-to-steel double strap joint increases the glass transition temperature by 30% and thus, the bond strength was increased at moderately elevated temperatures by about two fold compared to neat epoxy. Han and Fina [22] found that the aggregation of CNTs into bundles or ropes in the sonicated polymers and the high interfacial thermal resistance caused by the phonon mismatch are critical issues accompanied with CNTs as thermally conductive fillers in polymer composites. Therefore, in this study, the parameters of the sonication process were carefully selected to achieve the best dispersion of CNTs in the adhesive material.

Improving the impact performance of the SAJs via introducing nanofilers has not studied yet. Accordingly, the main objective of the present work is to evaluate the performance of SAJs modified with multi-walled carbon nanotubes (CNTs) under flexural and thermo-mechanical impact loads. Carbon fiber reinforced epoxy (CFRE) composite adherends were tapered at 15° and adhesively bonded using Epocast 50-A1/946 adhesive, which primarily developed for joining and repairing of composite aircraft structural components. The SAJs were modified with the optimum percentage of 0.5 wt% CNTs, which was carefully dispersed into the adhesive material using Ultrasonic Processor. The performance of SAJs was measured under thermo-mechanical impact loads. Drop weight impact tests were performed at room temperature (25°C), +50°C and +75°C temperatures in accordance with ASTM D 7136. Three-point impact tests were performed to characterize the residual strength after impact of the joints and the results were compared with the flexural strength of fresh specimens. The scarf adhesive joints (SAJs), which are bonded by neat epoxy (NE) and multi-walled carbon nanotube (MWCNT), will be designated as NE-SAJs and CNT-SAJs respectively.

2. Experimental Work

2.1. Materials

Multi-Walled Carbon Nanotubes (CNTs) with outer diameter less than 8 nm, inner diameter in the range of 2-5 nm, and length of about 30 μm were used to modify the epoxy adhesive. The CNTs were manufactured by Timesnano, Chengdu Organic Chemicals Co. Ltd, Chinese Academy of Sciences with purity higher than 95 wt%. The adhesive was manufactured by Huntsman Advanced Materials Americas Inc., for joining and repairing of composite aircraft structures. The glass transition temperature of the Epocast 50-A1/946 adhesive system, as provided by the manufacturer, is 72°C. The adherends of the SAJs were cut from carbon fiber reinforced epoxy (CFRE) composite laminates with an area of 500x500 mm^2 and thickness of 5±0.1 mm. The composite laminates were manufactured from 25 layers of plain woven carbon fiber fabrics (T300-3k, 200 g/m^2) and epoxy matrix (YPH-120-23A/B, manufactured by CHN Carbon Fiber Technology Co. Ltd) using prepreg technique with a curing cycle of 70℃ for 2.5 hours. The adherends were bonded using a two-component thermoset epoxy adhesive, Epocast 50-A1/946, with a mixing ratio (by weight) of 100:15. The mechanical properties of the CFRE adherends are illustrated in Table 1.

Table 1. Mechanical properties of the adhesives and plain woven carbon fiber composite adherends [5]

Properties	Materials		
	NE	0.5 wt% MWCNT/E	CFRE adherends
Tensile strength (MPa)	75.53	81.21	895.28
Tensile modulus (GPa)	3.43	4.06	81.66
Poisson's ratio	0.32	0.313	0.052
Shear strength (MPa)	50.71	53.51	145.41
Shear modulus (GPa)	1.45	1.60	6.94

2.2. Fabrication of the SAJs

The fabrication procedures of the scarf adhesive joints (SAJs) were reported earlier in details by Khashaba et al. [5-7] and are summarized in the coming subsections.

2.2.1. Preparation the tapered adherends. The CFRE laminates (500x500 mm^2) were cut into 500x125 mm^2 adherend panels using diamond bench saw. Scarf angle of 15^o was machined into the longest dimension of the adherend (500-mm), Fig. 1a, using a 46-grit Al_2O_3 vitrified cut-off wheel, which result in good surface finish [23]. As the tapered section has lower stiffness toward the tip, a 10 mm-thick steel back plate was used to support the panel, during tapering process, against out-of-plane deflection [5]. The tapered surfaces were cleaned by wiping them with *acetone-dampened cloth* as recommended by ASTM D 2093. This step is important for removing any contaminations from loosely held debris that can result from the cutting process. To ensure drying of the mating surfaces, the tapered sides were left upwards for 2h in a clean, dust-free area.

2.2.2. Preparing the adhesive materials. The optimum weight percentage of 0.5wt% CNTs was determined previously by Khashaba et al. [3] and used in this study to enhance the adhesive layer using Ultrasonic Processor with a maximum power of 750 W. The sonication amplitude was fixed at 375W (50% of the maximum apparatus power) for 30 min in order to reduce the damage of CNTs during dispersion in a volume of 150 cm^3 of the epoxy adhesive. These sonication conditions were corresponding to an energy density of 4500 W·s/ml, which is suitable for dispersion of CNTs in the Epocast adhesive [5,6]. The mixture's temperature was kept less than or equal to 50°C via temperature probe, which is fixed at the maid distance between the sonicator probe (25-mm diameter) and the beaker wall. Sonication at temperature of about 50°C reduces the mixture viscosity, which yields better dispersion of CNTs in the epoxy adhesive without degrading their mechanical properties. The mixture was evacuated to remove any air bubbles at 40°C and pressure of -133 Pa for one hour using drying vacuum oven model DZF-6050. The well dispersed CNTs in the adhesive epoxy were confirmed by Khashaba et al. [3] through scanning electron microscope image analysis. The mechanical properties of the Epocast epoxy adhesive and the modified adhesive with 0.5 wt% CNTs are illustrated in Table 1.

2.2.3. Assembly procedures of the SAJs. The neat and the modified Epocast adhesive were employed to fabricate the SAJs in CFRE composites with a bondline thickness of 0.25 mm. A pair of foil gages was bonded at the ends of the tapered surface of one adherend to maintain a constant bondline thickness of 0.25-mm as shown in Fig. 1a. The hardener 946 (epoxy Part-B) was gradually added to Epocast 50-A1 adhesive (epoxy part-A) and manually stirred for 5 minutes. The modified Epocast 50-A1 adhesive with CNTs should be cooled to room temperature after the evacuation (at

40°C) and before adding the hardener. This is because the Epocast 50-A1/946 has low gel time (20 min at 25°C) and accordingly, the temperature of the evacuated mixture (40°C) leads to decreasing the gel time as well as accelerating the curing process. In addition, it increases the possibility of voids as a result of increasing the exothermic heat of curing reaction.

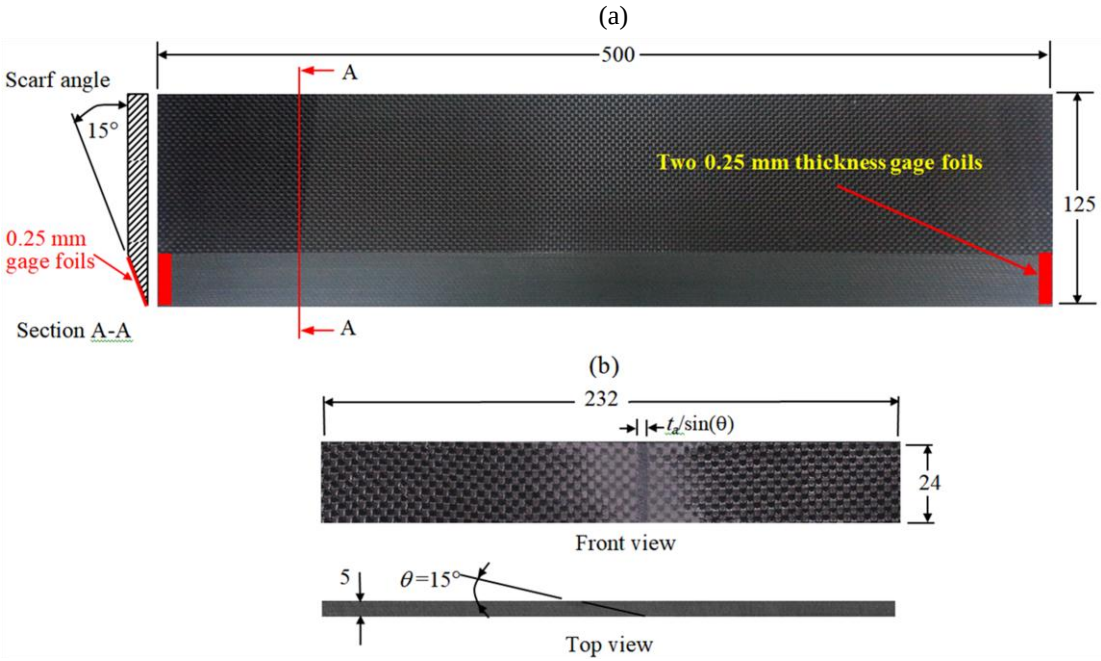

Figure 1. Images of: (a) The machined adherends (500x125 mm), and (b) front and top views of the SAJ with 15° scarf angle.

Subsequently, the adhesive was spread on both mating tapered surface of the parent adherends. The mating surfaces were accurately assembled on waxed glass plate. The adherends were prevented from slipping on each other using two 3-mm thick glass strips. These strips are bonded on the glass plate ahead of the non-tapered adherend ends. A second waxed glass plate was placed on the top surface of the assembled adherends. To squeeze out the excess adhesives, the assembly was compressed by dead weights of 50 kg, which were distributed on the upper glass plate. The assembly was kept for 10 days at 25°C aiming at complete curing of the adhesive material.

The final length (L) of the assembled panels is given by:

$$L = 2(125) + \frac{t_a}{\sin\theta} - \frac{t}{\tan\theta} \quad (1)$$

where t is the adherend thickness (5 mm), t_a is the adhesive thickness (0.25 mm), and θ is the scarf angle, Fig. 1. The length of the SAJs with scarf angles of 15° is 232 mm. A computer-controlled abrasive waterjet machine was used to cut the bonded panels into the SAJs with dimensions of 232x24x5 mm^3, Fig. 1b. The abrasive waterjet technique is selected to avoid the harmful effect of the induced temperature in traditional cutting processes of FRP composites.

2.3. Impact Tests

The fabricated SAJs were tested against low-velocity impacts using a drop-weight testing machine (model CEAST 9340), Fig. 2a. The impact tests were performed at room temperature (RT) of 25°C, and at hot temperatures of 50°C and 75°C according to ASTM D 7136. The selected test temperature of 50°C simulates the summer midday temperature of some countries. Performing impact tests at

temperature of 75°C was used to investigate the possible effects of temperature rise close to the adhesive T_g. The temperature was controlled using a thermal conditioning chamber of the drop-weight testing machine, figure 2. The hot air inside the chamber being circulated and distributes by a fan, figure 2b.

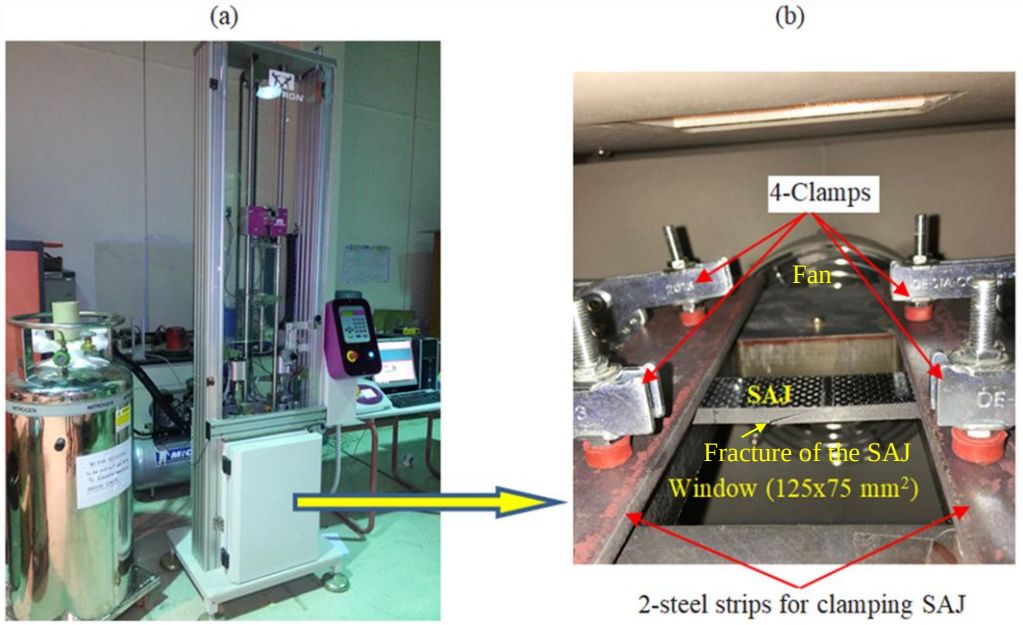

Figure 2. (a) Falling weight impact tester model CEAST 9340, and (b) specimen clamped inside thermal conditioning chamber of impact tester.

The SAJs were subjected to the selected test temperature (50°C or 75°C) for at least 45 min, before clamping the specimen. This time is enough to ensure homogenous distribution of the temperature across the thickness of the SAJs, which assisted by their lower thermal conductivity (4.6-0.42 W/m°C) compared with some important engineering materials such as steel (= 53 W/m°C), brass (= 109 W/m°C) and Aluminum (= 210 W/m°C) [24]. The upper tapered surface of the SAJs was marked and accurately centered against a steel plate having a rectangular window of 125x75 mm^2. This yields a 75 mm long span. The SAJs were constrained clamped-clamped via two-steel strips, which were pressed via four-clamps of the testing machine as shown in Fig. 2b.

The SAJs were subjected to thermo-mechanical impact loads at energy of 1.25 J. The impact energy of 1.25 J was selected based on preliminary tests, which enough to collapse the joints at RT. At 75°C, the SAJs are not fractured and thus, additional impact tests were performed at impact energy of 2.27J. The impact tests were performed via hemispheric impactor of 16 mm in diameter. The testing machine was equipped with a pneumatic anti-rebound device that mainly used to prevent secondary impact on specimen when tup rebounds after impact. Three SAJs were tested for each adhesive type (NE and CNT/E) and temperature degree (25°C, 50°C and 75°C).

In general any material fixed as clamped-clamped and subjected to temperature it will be expand and may be bend due to buckling. In the present study, the adherends of the SAJs is made from woven CFRP composite with approximate zero (or negative) axial coefficient of thermal expansion (CTE) of the yarns, which can effectively restrict the in-plane thermal displacement motions of epoxy resin [25]. The CTE of some important engineering materials are: -0.1 for carbon fiber, 5-6 for glass fiber, 12 for steel and 24 for aluminum (10^{-6}/°C). Accordingly, the carbon fiber adherends of the SAJs have approximately zero thermal expansion, no buckling and remained straight without any deformation before applying the thermal-impact load.

The values of the falling height and impact velocity were automatically evaluated by the machine software. However, they can be determined from Eqs. (2) and (3), respectively, as follows:

$$H = \frac{E_i}{mg} \tag{2}$$

$$v_i = \sqrt{\frac{2E_i}{m}} = \sqrt{2gH} \tag{3}$$

where E_i is the impact energy (1.25 J and 2.27 J), v_i is the impact velocity (0.892 m/s and 0.897 m/s, respectively), H is the drop-height of the impactor (41 mm), m is the total mass of the impactor (3.132 kg and 5.632 kg, respectively) and g is the gravity acceleration (g = 9.81 m/s^2).

Knowing the contact force and the impact velocity, the impactor acceleration $a(t)$, velocity $v(t)$, displacement/deformation $u(t)$, and energy $E(t)$, respectively, were calculated in terms of time, as follows [26]:

$$a(t) = \frac{P(t)}{m} - g, \tag{3}$$

$$v(t) = v_i - \int_0^t a(\tau)d\tau = v_i - \int_0^t \frac{p(\tau)}{m}d\tau, \tag{4}$$

$$u(t) = \int_0^t v(\tau)d\tau \tag{5}$$

$$E(t) = \int_0^t P(\tau)du = \int_0^t P(\tau)v(\tau)d\tau \tag{6}$$

where $E(t)$ is the total energy transferred from the impactor to the specimen at an instant t. A part of $E(t)$ is dissipated (absorbed) through several damage mechanisms. Another part is stored as elastic energy within the specimen and is restituted back to the impactor as residual or rebound kinetic energy. By subtracting the rebound energy (E_r) from the impact energy (E_i = ½ $m\,v_i^2$) it is possible to calculate the absorbed energy (E_a). The residual energy is considered as the energy of the impactor when it rebounds and loses contact with impacted plate, i.e., when the force decreases back to zero. Hence, the absorbed energy (E_a) is evaluated as the asymptotic value of the energy $E(t)$ [24]. In most of the performed tests, the specimen collapsed before it could restitute back the elastic energy to the impactor. In such case, the absorbed energy cannot be evaluated and thus, the energy at failure is determined instead. In addition, the maximum contact force, the displacement at maximum contact force and the impact bending stiffness were also determined from the load-displacement curves.

2.4. Flexural Tests

Three-point-bending tests were performed on the SAJs at room temperature using servo-hydraulic universal testing machine (model Instron 8872, 10 kN). The bending tests were carried out at constant cross-head speed of 1.0 mm/min. The support span (75mm, Fig. 3) is closed to the recommended optional span-to-thickness ratio of 16:1, ASTM D7264. This optional span value was selected to simulate the support-pan (75mm) of the impact tests in which the specimens were clamped on a rectangular window of 125x75 mm^2. The residual bending properties were determined for the non-collapsed impacted specimens, especially which were tested at temperature of 75°C and impact energy of 1.25J. The loading roller was located on the center of the marked tapered surface of the impacted SAJs. For each test, the force and the cross-head displacement were recorded. Subsequently, the (residual) flexural stiffness, the maximum force at failure and the deflection at failure were determined.

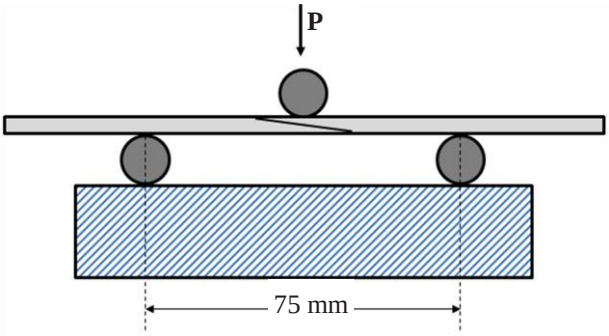

Figure 3. Schematic of three-point bending test of the SAJs.

3. Results and discussion

3.1. Load-displacement curves

Figures 4 and 5 show samples of load-displacement curves and energy-time curves of respectively the NE-SAJs and CNT-SAJs in drop-weight impact tests at 1.25J and different temperatures. The main characteristic of the load-displacement curves at room temperature (RT) of 25°C and at 50°C is the elastic-brittle behavior of both NE-SAJs and CNT-SAJs. The force increases almost linearly due to the viscoelastic behavior of the adhesive as well as the adherends, which have stiffness variation (lowest toward the tip). The slope of the linear portion of the load-displacement curve starts to decrease at about 80% of the maximum contact force due to disbonding in the bond line region of the scarf joint [12]. A small portion of the absorbed energy is dissipated by material damage (demonstrated by the decrease of the slope of the linear portion of the load-displacement curve at higher contact force). The absorbed energy was stored as the elastic strain energy and converted to kinetic energy after brittle fracture.

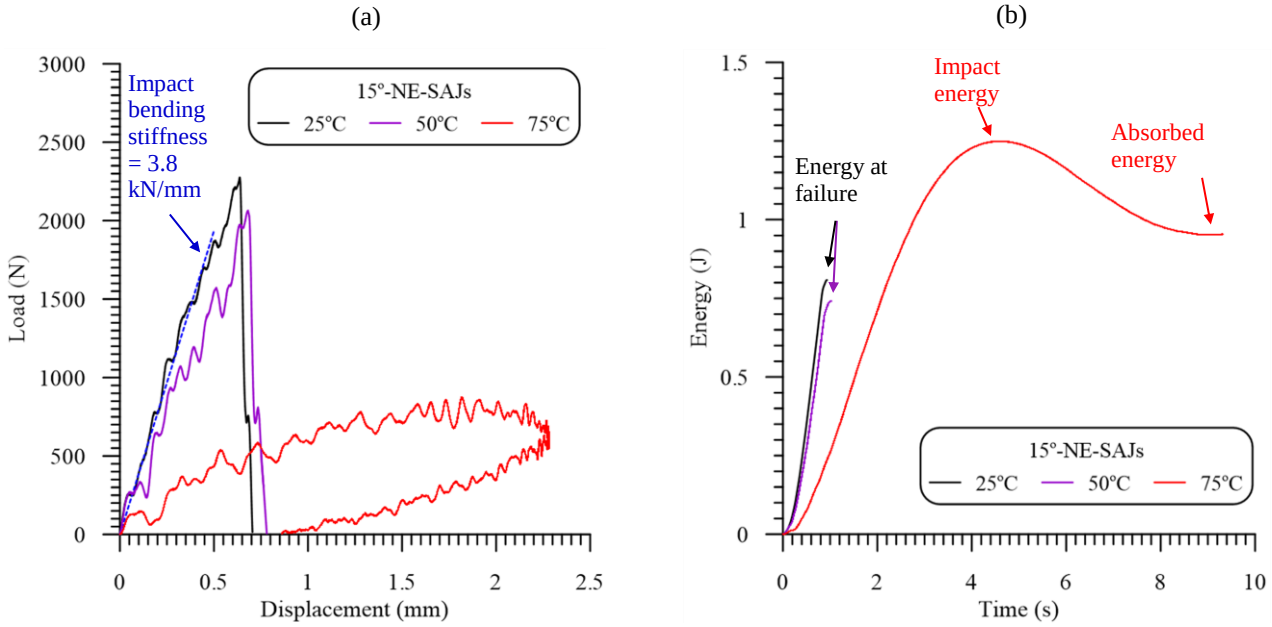

Figure 4 (a) Load-displacement curves, and (b) Energy-time curves of the NE-SAJs at 1.25 J

A sudden drop to zero-force was observed at the maximum contact force, demonstrating a brittle failure (fracture) of the SAJs and provides a measurement of a maximum contact force and the displacement at maximum force. This behavior was attributed to the elastic-brittle behavior of either the bulk adhesive [3,27] or the SAJs [5-7] in tensile tests at RT. Moreover, the load-displacement curves of the CFRE laminates, in low-velocity impact tests, showed an elastic-brittle behavior at RT and 50°C [24]. Khashaba and Othman [24] have reported that increasing the temperature from RT to 50°C has insignificant effect on low-velocity impact damage resistance of CFRE laminates.

The load-displacement behavior of the NE-SAJs and the CNT-SAJs at 75°C is characterized by hysteresis curves accompanied with large displacements as well as lower impact bending stiffness, which means the viscosity is the main source of energy absorption, as shown in Figs. 4a and 5a, respectively. This behavior was attributed to the softening of the adherends and the adhesive layer, which has glass transition temperature (72°C) slightly lower than the test temperature. The energy-time curves of the NE-SAJs and the CNT-SAJs at 75°C behave almost in the same manner as shown in Figs 4b and 5b respectively. The total impact energy (1.25 J) is first transferred to the joint. It is stored as elastic energy and non-elastic damage energy. The NE-SAJs and the CNT-SAJs absorb energy of about 65% of the impact energy (1.25 J) in the form of damages and leaving elastic energy of about 35%, which is dissipated in the rebound of the impactor. The joints under such test conditions (impact energy of 1.25 J and test temperature of 75°C) are not collapsed and thus, the residual flexural properties are measured and compared with those of fresh SAJs as will be seen later. To measure the failure properties of the SAJs, new impact tests are performed at impact energy of 2.27 J and test temperature of 75°C and the results are compared with those carried out at 1.25 J.

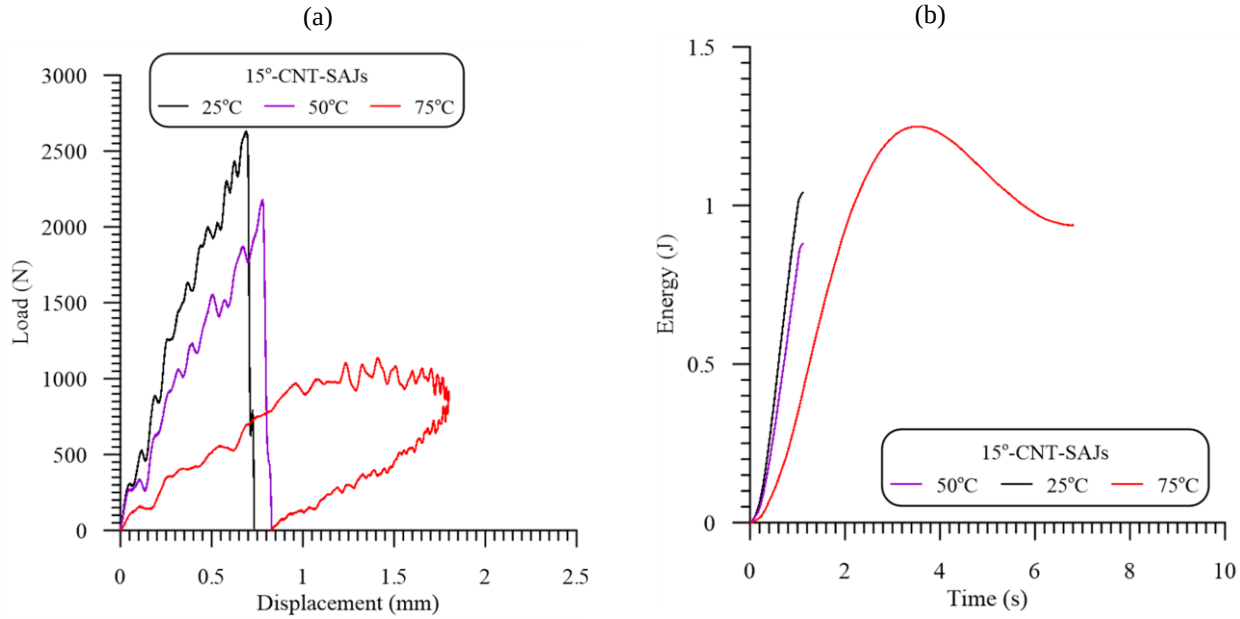

Figure 5 (a) Load-displacement curves, and (b) Energy-time curves of the CNT-SAJs at 1.25 J

Figure 6a and b shows respectively samples of the load-displacement and energy-time curves of both NE-SAJs and CNT-SAJs at impact energy of 2.27 J and test temperature of 75°C. The first region of the load-displacement curves of the SAJs typically behave almost linearly, up to a displacement of about 0.5 mm, followed by a nonlinear elastic behavior accompanied with brittle catastrophic fracture at maximum contact load, Fig. 6a. The displacements at maximum contact loads are nearly three times

larger than that tested at 1.25 J, Figs. 4a and 5a. The CNT-SAJs have higher impact bending stiffness, larger contact force and lower displacement at maximum contact force compared with those of the NE-SAJs as shown in Fig. 6a. One NE-SAJ was not fractured at 2.27 J and accordingly, has a hysteresis load-displacement behavior and energy-time curve with rebound energy of 23% and absorbed energy of 77% as shown in Fig. 6b. It is interesting to note that the load-displacement curves of the fracture and not fractured NE-SAJs have almost the same behavior up to the maximum contact load (at displacement of 2.65 mm).

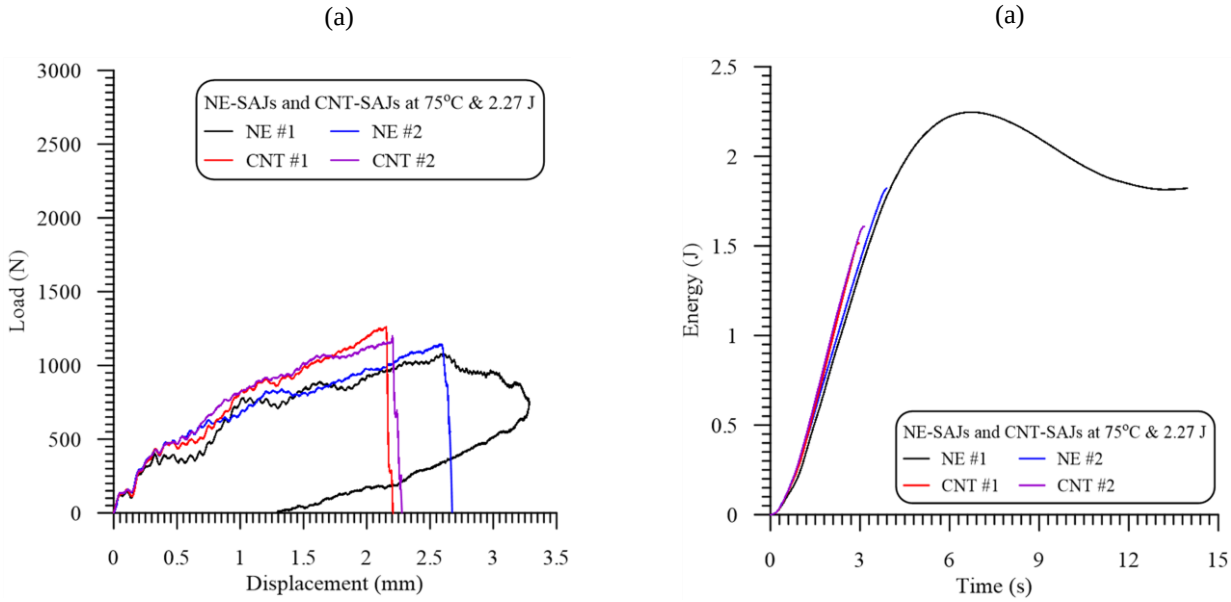

Figure 6. (a) Load-displacement curves, and (b) Energy-time curves of the CNT-SAJs at 75°C and 2.27 J

3.2. Effect of CNTs

The impact bending stiffness, maximum contact force and displacement at maximum contact force are measured directly from the load-displacement curves and the average value of three tests, for each condition, are presented vs temperature as shown in Figs. 7a, 8a and 9a, respectively. The impact bending stiffness values in Fig. 7a were measured from the slope of the initial linear portion of the load-displacement ascending curves of Figs. 4a and 5a. Impact bending stiffness has been known to be an important property in assessing the damage resistance of composite materials in particular to delamination [28].

Figures. 7a, 8a, 9a and 10a shows the infusion effects of optimum percentage of (0.5 wt%) CNTs into the adhesive layer on the impact bending stiffness, maximum contact force, displacement at maximum contact force and energy respectively at different temperatures. The results in Figs. 7a to 10a include also the standard deviation and the gain/loss percentages in the impact properties of the CNT-SAJs compared with the NE-SAJs. The gain/loss percentages in the impact bending stiffness, maximum contact force, displacement at maximum contact force and energy at 50°C and 75°C are also estimated and compared with those at room temperature of 25°C as shown respectively in Figs. 7b, 8b, 9b and 10b.

It is evident from Fig. 7a that incorporation of CNTs into the epoxy adhesive increases the impact bending stiffness of the CNT-SAJs by 8.3%, 7.4% and 11.8% compared with the NE-SAJs at test

temperatures of 25°C, 50°C and 75°C respectively. Accordingly, the maximum contact force of the CNT-SAJs, at these test temperatures, was increased by 15.6%, 21.3% and 18.9% respectively as shown in Fig. 8a.

The improvement of the impact bending stiffness as well as the maximum contact force in drop weight impact tests was due to the reinforcing effects of high strength CNTs (63 GPa to 200 GPa [17]) on the increased mechanical properties of the adhesive material as shown in Table 1. Moreover, incorporation of CNTs into the adhesive layer can activate interfacial mechanisms at the nanoscale, which can play a key role in arresting crack propagation and accordingly, increasing the local stiffness of the SAJ [25]. Alnefaie et al. [29] reported that the failure strain of CNT-nanocomposite was lower than those of the neat epoxy by 18.9%. The mechanical interlocking of the adhesive layer with the debonded carbon fibers (CFs) that superimposed on the valley and peaks of the machined tapered surfaces, may be more effective for the modified adhesive with CNTs and thus, increasing the mechanical properties of their joints [6,30].

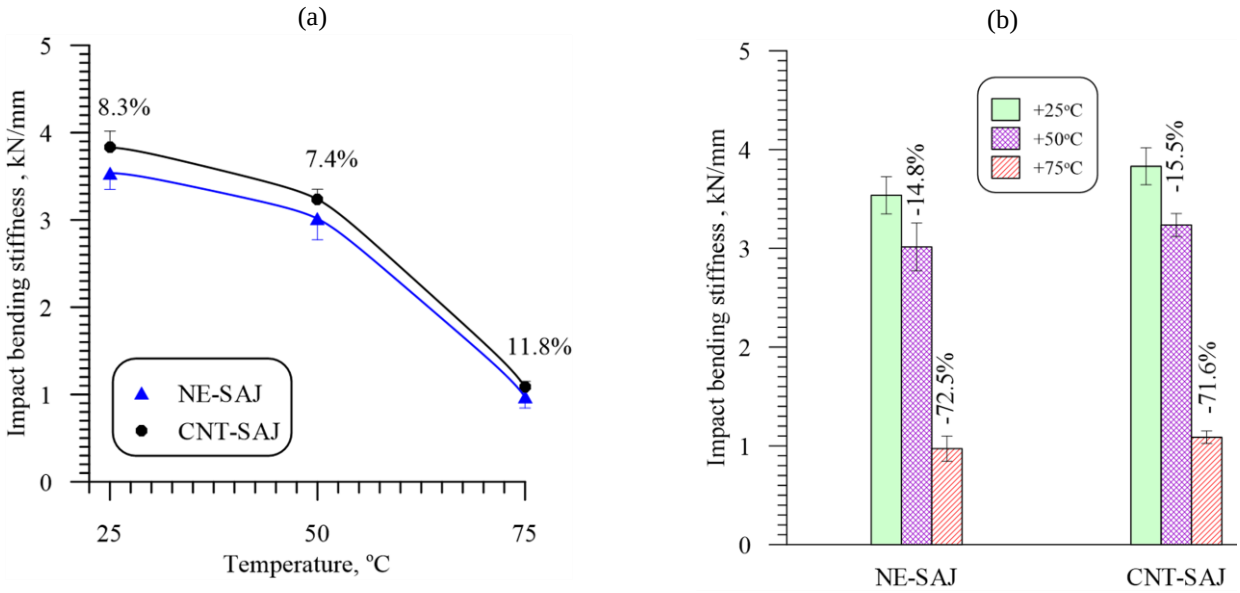

Figure 7. Gain/loss percentage of the stiffness: (a) effect of CNTs, and (b) effect of temperatures.

In addition, Khashaba et al. [5-7] showed improvement ranging from 12% to 39.6% in the ultimate tensile strength of the CNT-SAJs with scarf angles reanging from 5° to 45° compared with those of the NE-SAJs. In particular, the ultimate tensile strength of the 15°-CNT-SAJs was (91.88 MPa) improved by 21.9% compared with those of the NE-SAJs (75.39 MPa) [5].

The higher contact force of the CNT-SAJs is compensated by their higher impact bending stiffness and accordingly, the CNTs don't seem to be influencing the displacement at maximum contact force of the SAJs as shown in Fig. 9a. The results in this figure showed that the gain/loss in the displacements at maximum contact force of the CNT-SAJs were 5.3%, 2.8% and -6.6% at test temperatures of 25°C, 50°C and 75°C respectively.

The energy-time curves in Figs. 4b to 5b were obtained directly from the PC of the testing machine and can also be estimated from the area under the load-displacement curves [14]. The measured energy at 25°C and 50°C in these curves is the maximum energy at failure (zero loads). Because of the SAJs are not fractured at temperature of 75°C, the absorbed energy was determined at zero load after rebounding the impactor.

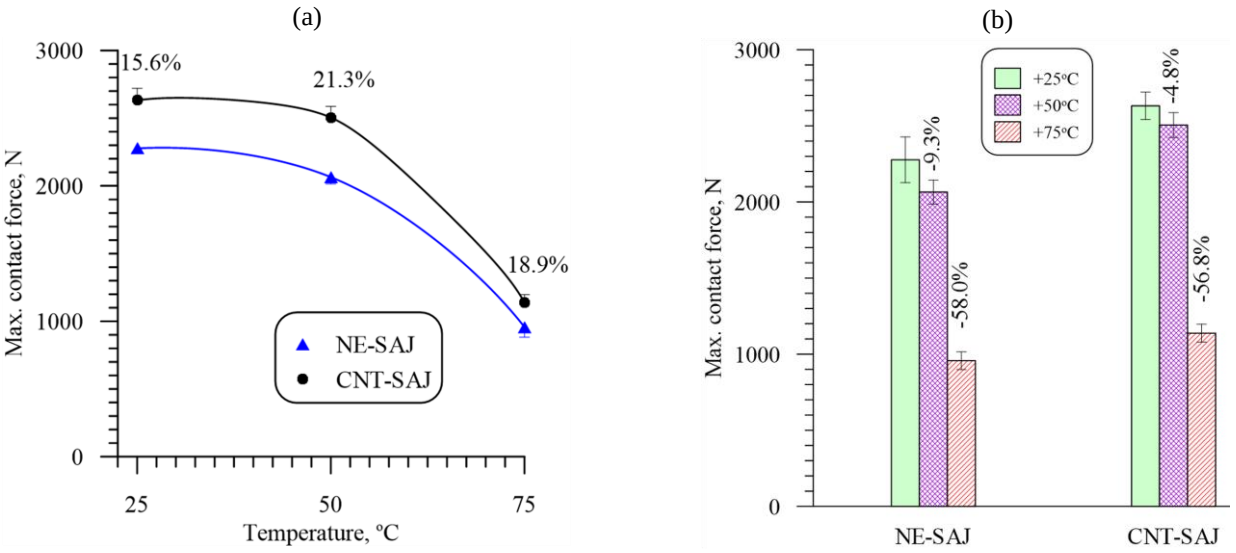

Figure 8. Gain/loss percentage of the maximum contact force: (a) effect of CNTs, and (b) effect of temperatures.

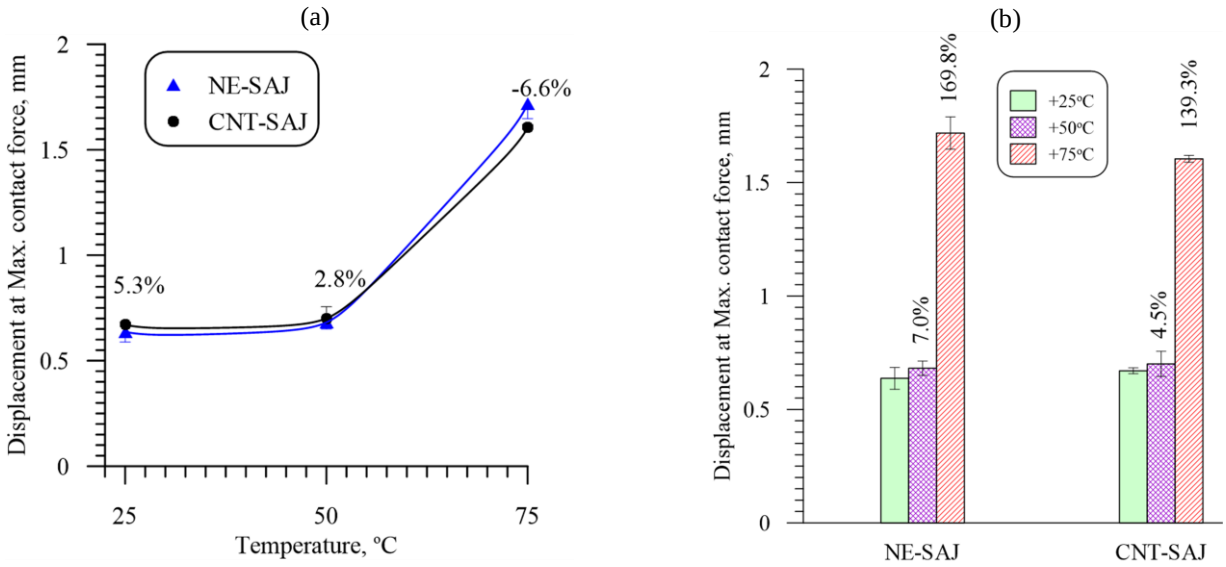

Figure 9. Gain/loss of the displacement at maximum contact force: (a) effect of CNTs, and (b) effect of temperatures.

Figure 10a shows the effect of the CNTs on the energy of the SAJs at different temperatures. The results in this figure showed that the incorporation of CNTs into the adhesive layer of the SAJs improves their energy by 15.2% and 16.4% respectively at temperatures of 25°C and 50°C. The higher energy of the CNT-SAJs at 25°C and 50°C can be interpreted with the aid of the CNTs ‘‘stick-slip’’ motion [25,31,32], which is responsible for the improvement of energy dissipation capability of CNT-SAJs. During impacting the CNT-SAJ, an interfacial shear stress is generated between the CNTs and the surrounding epoxy due to the elastic mismatch according to the well–known shear lag theory. At small contact loads, the nanotubes will elongate together with the matrix. Once the contact load

exceeds a critical value, the impact bending displacement will be increased and thus the nanotubes will stop elongate together with the matrix [32]. Further increasing of the contact load will result in increasing the dissipated energy through the slippage between the nanotubes and the matrix [29,32].

The increase in the absorbed energy of the CNT-SAJs was also assisted by the improving of fracture toughness mode-I and mode-II of FRP composites modified by CNTs [33,34]. Karapappas et al. [33] found a significant increase in the load bearing ability as well as in the fracture energy for both Mode-I and Mode-II of the modified epoxy matrix with CNTs. Quan et al. [34] reported that incorporation of 0.5wt% MWCNTs to bulk epoxy and CFRPs improves the mode-I fracture energy by 15.2% and 8.2% respectively compared with the control materials. In addition, mode-II fracture energy of bulk epoxy and CFRPs were dramatically enhanced by 60.0% and 68.1% respectively. They attributed the improvement in both mode-I and mode-II fracture energy of the modified bulk epoxy and FRP composites to MWCNT pull-out, crack bridging, nanotube breaking and crack deflection.

At temperature of 75°C the CNTs have insignificant effect on the absorbed energy due to the lack of pull-out resistance of the debonded CNTs from the epoxy adhesive. This was attributed to the fact that the mechanical properties of the polymer matrices are highly degraded at test temperature closed to their T_g.

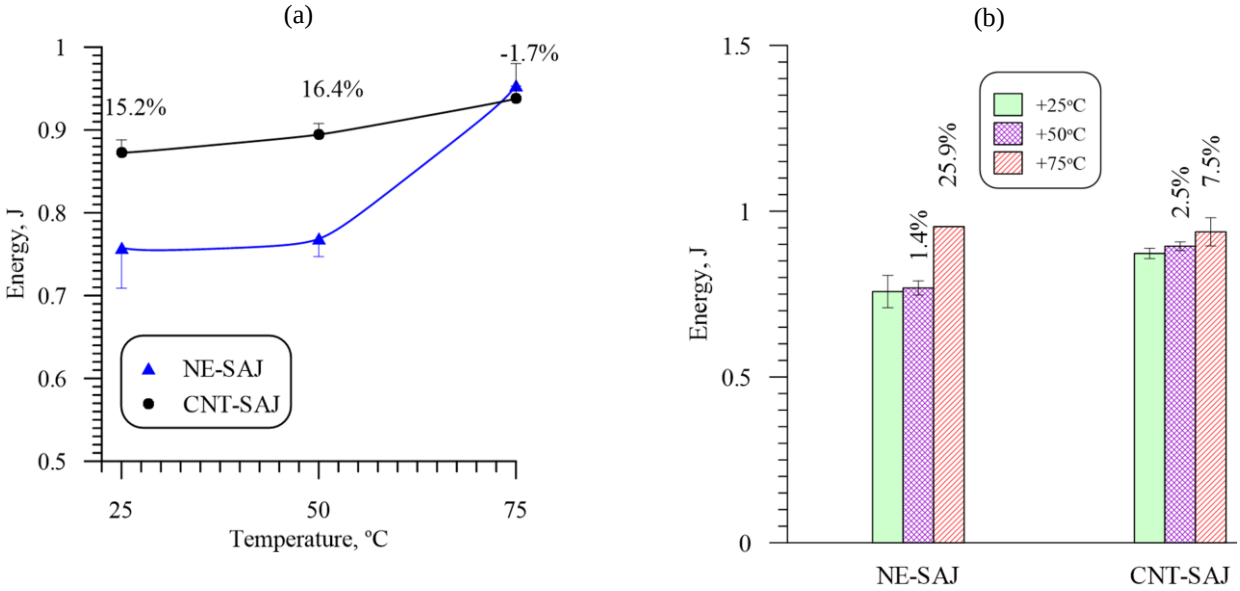

Figure 10. Gain/loss percentage of the energy: (a) effect of CNTs, and (b) effect of temperatures.

3.3. Effect of test temperature

The effect of test temperature on the impact bending stiffness, maximum contact force, displacement at maximum contact force and energy of the SAJs is illustrated respectively in Figs. 7b, 8b, 9b and 10b. The gain/loss percentages in these figures were calculated for the impact properties at test temperatures of 50°C and 75°C relative to those at RT of 25°C.

It is evident from Fig. 7a that the impact bending stiffness of the SAJs decreases significantly with increasing the test temperatures and thus the maximum contact force, Fig. 8a. On the contrary, the displacement at maximum contact force was evidently increased, Fig. 9a, as a result of decreasing the joint impact bending stiffness. At 50°C, due to the softening and ductility of the specimens, the impact bending stiffness of the NE-SAJs and CNT-SAJs is moderately decreased by respectively 14.8% and 15.5%, Fig. 7b. Accordingly, the maximum contact force of the NE-SAJs and CNT-SAJs was respectively reduced by 9.3% and 4.8%, Fig. 8b, and the displacement was increased by 7% and 4.5%, Fig. 9b, compared with those tested at RT.

The temperature effects on the impact properties of the SAJs are aggravated at 75°C. The results in Fig. 7b showed that the impact bending stiffness of the NE-SAJs and CNT-SAJs at test temperature of 75°C was drastically decreased by about 72.5% and 71.6% respectively and thus, the maximum contact force was eventually decreased 58% and 57%, Fig. 8b, compared with those tested at RT. Indeed, it is widely reported that stiffness, yield stress and strength of polymers significantly drop near glass transition temperature [35]. On the other hand, the displacements of the NE-SAJs and CNT-SAJs were dramatically increased by 170% and 139%, respectively, compared with those tested at RT as shown in Fig. 9b. Decreasing the maximum contact force and increasing the displacement at maximum contact force as a result of decreasing the joint impact bending stiffness was clearly indicated in Fig. 11.

This result was attributed to the softening of the adhesive layer of the SAJs at 75°C and thus, the capacity to transfer the loads over the adhesive/adherends interfacial bond was decreased. It is believed that the constrained clamped-clamped SAJs subjected to elevated temperature will result in considerable and unavoidable initial strain states in the adhesive layer and thus, decreasing the impact properties of the joint under thermo-mechanical impact loads. The effect of temperature on the initial strain state along the adhesive layer is a new topic and remains open for further research. Nguyen et al. [11] reported that the ultimate load and stiffness of double strap steel/CFRP adhesively-bonded joints decreased by about 15%, 50% and 80% when temperatures increased by 0°C, 10°C, and 20°C above T_g, respectively. Agarwal et al. [36] have reported that to avoid failure of steel-CFRP single-lap joints under thermo-mechanical loads, the highest service temperature of the adhesive should be lower than its T_g value by about 30°C, which may agree with the results obtained at 75°C compared to those at RT and 50°C.

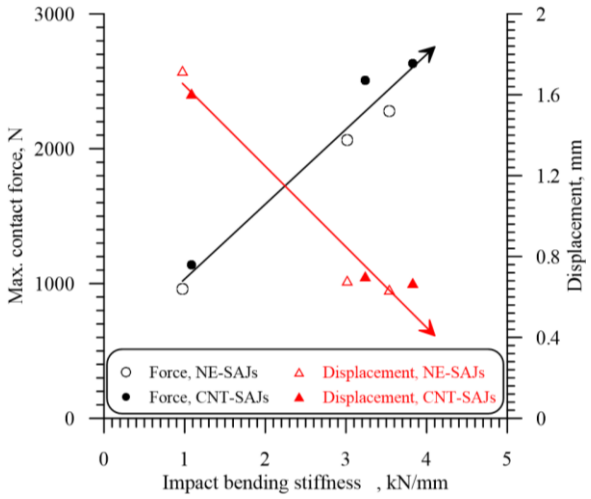

Figure 11. Force and displacement vs. stiffness of the SAJs

The energy at failure of the NE-SAJs and CNT-SAJs at test temperature of 50°C is marginally increased by 1.4% and 2.5%, respectively, compared with those tested at RT, Fig. 10b. This was attributed to the force-displacement curves of the SAJs at RE and 50°C is almost the same behavior. While at 75°C (slightly higher than T_g of the adhesive materials, 72°C), hysteresis loop behavior is observed, which means the viscosity is the main source of energy absorption. Regarding to the different ways of energy dissipation, it is inappropriate to compare the energy at failure at RT with the higher energy absorption at 75°C (25.9% and 7.5% respectively for NE-SAJs and CNT-SAJs, Fig. 10b). In that context, it is worth noting that at test temperature of 75°C, the CNTs have insignificant effect on the absorbed energy.

This result was due to the fact that the infusion of CNTs into the adhesive layer can play contrary roles in deciding the performance of the SAJs especially under various temperature environments for the following reasons: (a) improving the mechanical properties of the CNT-nanocomposites as shown in Table 1, (b) improving the glass transition temperature (T_g) of adhesive [16-19] and thus delay their softening temperature, (c) the difference in the coefficients of thermal expansion of the reinforcing carbon fibers, CNTs and the adhesive could be significant enough to cause considerable incompatible initial thermal strains along the adhesive layer between CFRP adherends and thus, microcracks initiation as well as interfacial shear failure before applying the impact loads, and (d) improving the thermal conductivity of the adhesive layer and thus, rapid distribution of the temperature with more softening and reduction of the adhesive strength. The thermal conductivity of multi-walled carbon nanotubes is (= 3000W/mK[20,21]) very high compared with epoxy adhesive (0.3 W/mK[21]) and some famous metals such as Aluminum (= 210 W/m°C).

Figures 12a and b shows a comparison between the fractured surfaces of the SAJs at RT and 75°C respectively. The fracture of the SAJs at RT was due to interfacial shear between the adhesive layer and the adherends, which initiated from the adherends tips and propagated toward the center of the tapered surfaces [5]. Cohesive failure of the adhesive layer was observed owing to jumping the interfacial failure from one interface to the other as shown in Fig. 12a. At 75°C the adhesive smearing the fractured surface of one tapered surface while, the adhesive layer was attached to the other tapered surface without cohesive failure of the adhesive layer as shown in Fig. 12b.

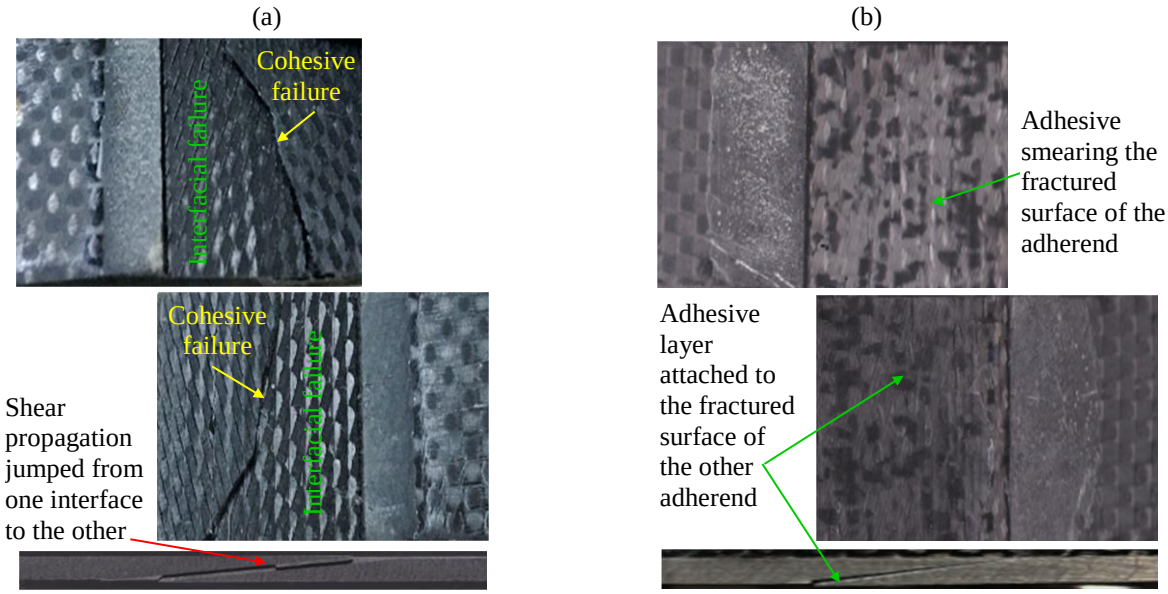

Figure 12. Images of fractured surfaces of the NE-SAJs: (a) at RT of 25°C (1.25J), and (b) at 75°C (2.25J)

3.4. Effect of impact energy

The effect of impact energy of 2.27 J on the failure properties of the SAJs was investigated at temperature of 75°C, where the joints are not collapsed under impact energy of 1.25 J. Fig. 13 shows the impact properties of both the NE-SAJs and CNT-SAJs at 2.27 J and 75°C. The results are compared with those tested at 1.25 J and 75°C and accordingly, the gain/loss in the impact bending stiffness, maximum contact force, displacement at maximum contact force and energy were illustrated in Fig. 13 (vertical percentages). This figure also shows the effect of CNTs on the gain/loss in the impact properties of the CNT-SAJs compared with the NE-SAJs (horizontal percentages between parentheses) at 75°C and 2.27 J.

The results in Fig. 13 showed that at 2.27 J, the impact bending stiffness of both the NE-SAJs and the CNT-SAJs are increased respectively by 25.1% and 13.7% and accordingly, the maximum contact force was increased by 16% and 8.2% compared with those tested at 1.25 J. As the impact energy is increased, the energy transferred to the SAJs before failure is also increased. Hence, at impact energy of 2.27 J the displacement at maximum contact force of the NE-SAJs and the CNT-SAJs was increased by 50.5% and 35.7% respectively compared with those tested at 1.25 J. The energy at failure of both the NE-SAJs and the CNT-SAJs was also increased at impact energy of 2.27 J by 91.1% and 66.6% respectively relative to that tested at 1.25J.

Although the CNTs at 2.27J and temperature of 75°C have slightly increased the impact bending stiffness of the CNT-SAJs (1.6% increase), the maximum contact force was increased (10.9%) and the displacement at the maximum contact force was decreased (-15.8%) compared with the NE-SAJs. Qualitatively, this behavior agrees with the stiffness effects of Fig. 11. On the other hand, the energy at failure of the CNT-SAJs was decreased by -14.3% compared with that of NE-SAJs. These results were probably due to the contrary role of the CNTs in deciding the performance of composite bonded joints especially at higher temperatures near the glass transition value (T_g). The higher thermal conductivity of the CNTs (= 3000W/mK) compared with that of the epoxy adhesive (0.3 W/mK), can increase their temperature and accordingly, decrease the resistance to pull-out the CNTs from the adhesive materials. The pull-out of the CNTs can be assisted by their small length 30 μm and the elastic mismatch between CNTs and adhesive.

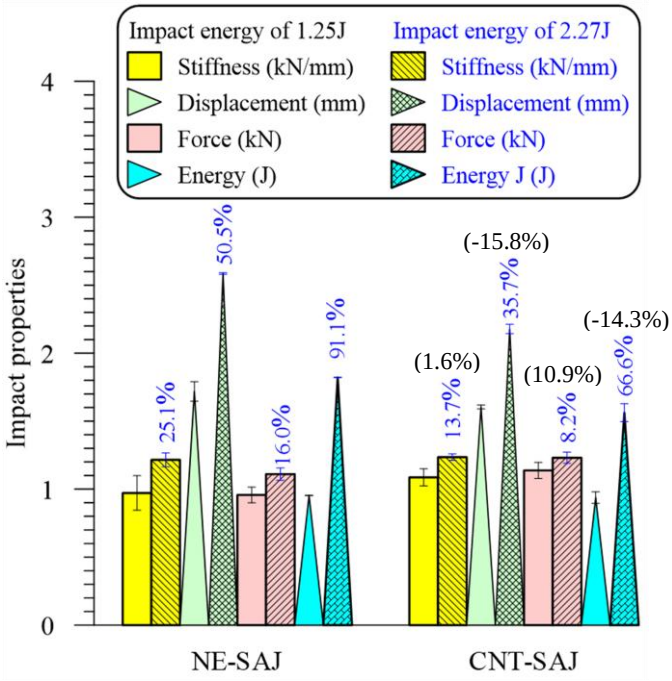

Figure 13. Effects of impact energy and CNTs on the impact properties of the SAJs at 75°C. The vertical percentages show the effect of impact energy, while the horizontal percentages show the effect of CNTs.

3.5. Bending results and discussion

Figure 14 shows a sample from the load-displacement curves of the NE-SAJs and CNT-SAJs in bending tests at RT. The main characteristics of these curves are the initial nonlinear small portion until intimate contact with the loading members of the three-point bending setup. The initial nonlinear region is followed by a linear relationship, which used to measure the flexural stiffness (modulus) of

the SAJs. The NE-SAJs were failed in catastrophic (brittle) manner owing to the interfacial failure of the adhesive layer, whereas almost of the CNT-SAJs exhibited interlaminar shear cracks that were initiated around the adhesive joint and propagated toward the specimen ends without adhesive failure. The initiation and propagations of the interlaminar cracks in the adherends of the CNT-SAJs can be demonstrated by the unstable load-displacement relationship up to the final fracture of the joint as well as visually examination of the joints during the bending test as shown in Fig. 14.

Figure 15 shows the flexural strength of fresh (new) SAJs as well as residual flexural strength after impact at 1.25 J and 75°C. The results in this figure showed that the incorporation of CNTs into the adhesive layer improves the flexural strength by 36.2%. The residual strength of the CNT-SAJs is (98.2%) higher than that of the NE-SAJs (86.1%). The reasons for the higher strength of the CNT-SAJs compared with the NE-SAJs were discussed in section 3.2. In addition to these reasons, the higher flexural strength accompanied with the interlaminar shear failure of the adherends without adhesive failure of the CNT-SAJs demonstrates the improvement in their interfacial shear resistance as a result of incorporating CNTs into the adhesive layer.

It is worth noting that although both of the impact and bending SAJs have the same gauge length (75 mm), the impact bending stiffness of the SAJs, Figs. 4a and 5a, is about two times higher than that determined through the bending tests at RT, Fig. 14. This result was attributed to the fact that the SAJs in the impact test can be considered as double-clamped beam, while in bending tests the joints were simply supported through the three-point tests setup. In addition, the loading rate in impact test is about fifteen times (14.9 mm/min) higher than that of the bending tests (1 mm/min). Challita et al. [37] reported a significant increase of the stiffness and strength of an epoxy bulk adhesive as the strain rate/loading velocity increases under compression and shear loadings. Based on the temperature-time superposition principle, it has been reported that [38] the increase in loading rate has a hardening effect similar to the effect of decreasing temperature of the viscoelastic materials, and accordingly increasing their stiffness.

The scatter in the flexural results of the fresh SAJs is less than that of the residual flexural properties (strength and modulus), which experienced different levels of impact damages before the flexural tests. The maximum scatter was observed in the residual tests of the CNT-SAJ, in which the final fracture is decided either by interfacial failure or interlaminar shear failure of the adherends. On the other hand, the minimum scatter was observed for the fresh NE-SAJs in which the interfacial shearing is the dominant failure mechanisms.

Figure 16 shows the effect of CNTs on the flexural modulus of the fresh as well as the residual strength after impact (at 1.25 J and 75°C) NE-SAJs and CNT-SAJs. The results in this figure showed that incorporation of CNTs into the adhesive layer has insignificant effect on the flexural modulus of the fresh CNT-SAJs compared with those of the NE-SAJs. The residual modulus of the NE-SAJs and CNT-SAJs has remarkable decreased to 71.7% and 81.3% respectively. This is because the residual flexural modulus depends on the damage level in the SAJs owing to the impact test, which greatly effect on the flexural stiffness of the joint and thus, the flexural modulus of the joint.

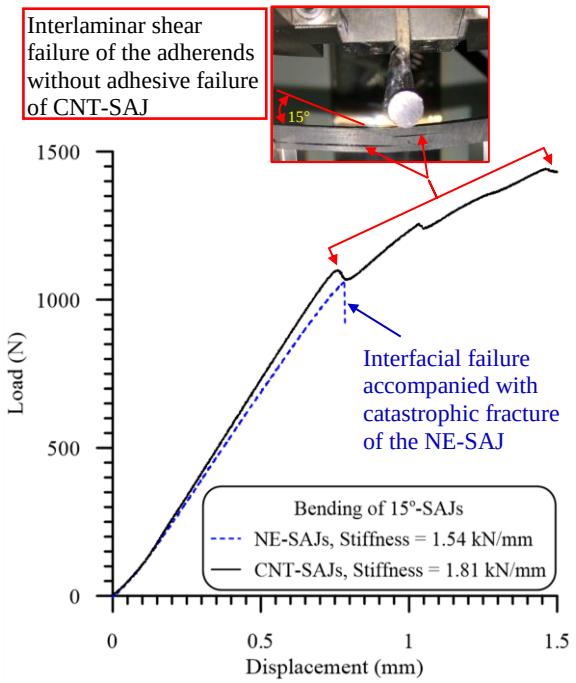

Figure 14. Load-displacement curves of fresh SAJs in bending tests

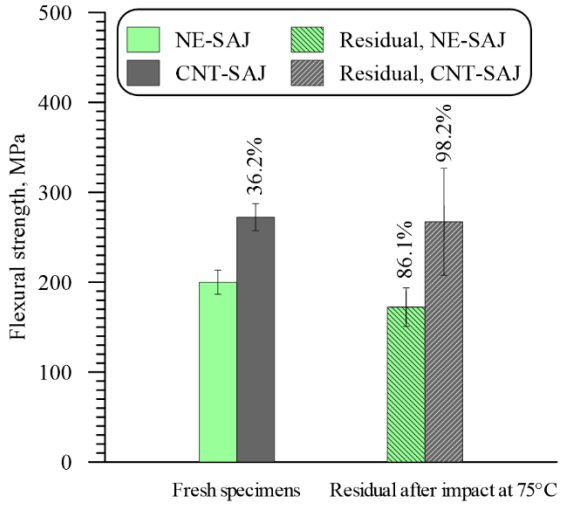

Figure 15. Flexural strength and residual strength after impact of the SAJs at 1.25 J and 75°C

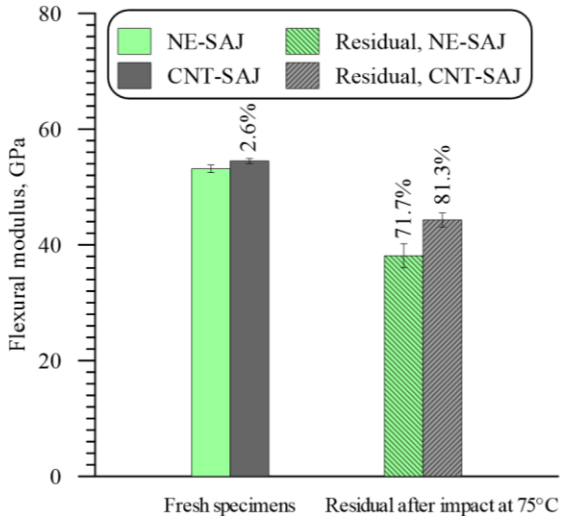

Figure 16. Flexural modulus and residual modulus after impact of the SAJs at 1.25 J and 75°C

4. Conclusions

In this work, an extensive experimental program was conducted to characterize the mechanical properties of scarf adhesive joints (SAJs) subjected to flexural and thermo-mechanical impact loads. Conclusions on the flexural properties as well as the effect of CNTs, impact energy, test temperature, on the impact bending stiffness, maximum contact force and absorbed/failure energy of the SAJs can be drawn as follows:

Effect of temperature: The main characteristic of the load-displacement curves (E_i = 1.25J) of both NE-SAJs and CNT-SAJs at room temperature (RT) of 25°C and 50°C is the elastic-brittle fracture involves the sudden drop to zero-force. While at 75°C, hysteresis loop behavior is observed, which means the viscosity is the main source of energy absorption. At this test temperature the impact bending stiffness of the SAJs was drastically decrease by about 72% and hence, the maximum contact force of the NE-SAJs and CNT-SAJs was drastically decreased by 58% and 57%, respectively. The energy at failure of the NE-SAJs and CNT-SAJs at test temperature of 50°C is marginally increased by 1.4% and 2.5%, respectively, compared with those tested at RT. Regarding to the different ways of energy dissipation, it is inappropriate to compare the energy at failure at RT and 50°C with the higher-energy absorption at 75°C (25.9% and 7.5% respectively for NE-SAJs and CNT-SAJs).

Effect of impact energy: To measure the failure properties of the SAJs at 75°C, new impact tests are performed at impact energy of 2.27 J and the results are compared with those carried out at 1.25 J. The results showed that as the impact energy is increased from 1.25 to 2.27 J, the impact bending stiffness, the maximum contact force, the displacement at maximum contact force are increased. As a consequence, the maximum energy transferred to the specimen is also increased. The CNT-SAJs have higher impact bending stiffness, larger contact force and lower displacement at maximum contact force compared with those of the NE-SAJs.

Effect of CNTs: Incorporation of CNTs into the epoxy adhesive increases the impact bending stiffness of the CNT-SAJs by 8.3%, 7.4% and 11.8% compared with the NE-SAJs at test temperatures of 25°C, 50°C and 75°C, respectively. Accordingly, the maximum contact force of the CNT-SAJs, at these test temperatures, was increased by 15.6%, 21.3% and 18.9% respectively. The energy at failure was of the CNT-SAJs improved by 15.2% and 16.4%, respectively at temperatures of 25°C and 50°C. In that context, it is worth noting that at test temperature of 75°C, the CNTs have insignificant effect on the absorbed energy due to the lack of CNTs pull-out resistance from the epoxy adhesive.

Flexural properties: The load-displacement curves and the visual examination of the SAJs in the flexural tests showed that the NE-SAJs were failed in catastrophic (brittle) manner owing to the interfacial failure of the adhesive layer. On the other hand, almost of the CNT-SAJs exhibited interlaminar shear cracks that were initiated around the adhesive joint and propagated toward the adherend ends without adhesive failure. The flexural strength of the CNT-SAJs is improved by 36.2% compared to the NE-SAJs. In addition, the residual flexural strength of the impacted CNT-SAJs at 1.2J and 75°C is (98.2%) higher than those of the NE-SAJs (86.1%). The residual modulus of the NE-SAJs and CNT-SAJs has remarkable decreased to 71.7% and 81.3% respectively.

Acknowledgements

This project was funded by the Deanship of Scientific Research (DSR), King Abdulaziz University, Jeddah, under grant no. G-196-135-38. The authors, therefore, acknowledges with thanks DSR for technical and financial support.

References

[1] Cheng X, Zhang J, Bao J, Zeng B, Cheng Y, Hu R. Low-velocity impact performance and effect factor analysis of scarf-repaired composite laminates. Int J Impact Eng 2017;111:85-93

[2] Nie H, Xu J, Guan Z, Wang Q, Li Z. Tensile Behaviors after Impact of Composite Scarf Joints. 7th International Conference on Mechanical and Aerospace Engineering (ICMAE), London, UK (2016) 9-16.

[3] Khashaba UA, Aljinaidi AA, Hamed MA. Nanofillers modification of Epocast 50-A1/946 epoxy for bonded joints. Chin J Aeronaut 2014;27(5):1288-300.

[4] Khashaba UA, Aljinaidi AA, Hamed MA. Development of CFRE composite scarf adhesive joints with SiC and Al2O3 nanoparticle. Composite Structures 2015;128: 415-427.

[5] Khashaba UA, Aljinaidi AA, Hamed MA. Analysis of adhesively bonded CFRE composite scarf joints modified with MWCNTs. Compos Part A-Appl S 2015;71: 59-71.

[6] Khashaba UA, Najjar IMR. Adhesive layer analysis for scarf bonded joint in CFRE composites modified with MWCNTs under tensile and fatigue loads. Compos Struct 184(2018)411-427.
[7] Khashaba UA, Aljinaidi AA, Hamed MA. Fatigue and reliability analysis of nano-modified scarf adhesive joints in carbon fiber composites. Compos Part B Eng 2017;120: 103-117.
[8] Khashaba UA. Static and fatigue analysis of bolted/bonded joints modified with CNTs in CFRP composites under hot, cold and room temperatures. Composite Structures 2018;194: 279–291
[9] Wheeler GE. Predicting Crack Growth Behavior in Adhesive Scarf Joints. BiblioBazaar, 2011.
[10] Jen Y-M. Fatigue life evaluation of adhesively bonded scarf joints. Int J Fatigue 2012;36:30-9.
[11] Nguyen TC, Bai Y, Zhao XL, Al-Mahaidi R. Mechanical characterization of steel/CFRP double strap joints at elevated temperatures. Compos Struct 2011;93(6):1604-12.
[12] Kim MK, Elder DJ, Wang CH, Feih S. Interaction of laminate damage and adhesive disbonding in composite scarf joints subjected to combined in-plane loading and impact. Composite Structures 94 (2012) 945-953
[13] Sato C, Ikegami K. Dynamic deformation of lap joints and scarf joints under impact loads. International Journal of Adhesion & Adhesives 2000;20: 17-25
[14] Ali M, Tan A, Joshi SC. Tailoring of bonded composite scarf joint interface for impact damage mitigation and stiffness Compatibility. Plastics, Rubber and Composites 45 (2016) 43-49.
[15] Ozdemir O, Oztoprak N. An investigation into the effects of fabric reinforcements in the bonding surface on failure response and transverse impact behavior of adhesively bonded dissimilar joints. Composites Part B: Engineering 126 (2017) 72-80.
[16] Korayem AH, Chen SJ, Zhang QH, Li CY, Zhao XL, Duan WH. Failure of CFRP-to-steel double strap joint bonded using carbon nanotubes modified epoxy adhesive at moderately elevated temperatures. Compos Part B Eng 2016;94:95-101.
[17] Korayem AH, Li CY, Zhang QH, Zhao XL, Duan WH. Effect of carbon nanotube modified epoxy adhesive on CFRP-to-steel interface. Compos Part B-Eng 2015;79: 95-104.
[18] Jiang C, Zhang J, Lin S, Ju S, Jiang D. Effects of free organic groups in carbon nanotubes on glass transition temperature of epoxy matrix composites. Compos Sci Technol 2015;118:269-275
[19] Gojny FH, Schulte K. Functionalisation effect on the thermo-mechanical behaviour of multi-wall carbon nanotube/epoxy-composites. Composites Science and Technology 2004;64: 2303–2308.
[20] Kim P, Shi L, Majumdar A, McEuen PL. Thermal transport measurements of individual multiwalled nanotubes. Phys Rev Lett 2001;87,215502/1-4.
[21] Sihn S, Ganguli S, Roy AK, Qu L, Dai L. Enhancement of through-thickness thermal conductivity in adhesively bonded joints using aligned carbon nanotubes. Compos Sci Technol 2008;68: 658-665
[22] Han Z, Fina A. Thermal conductivity of carbon nanotubes and their polymer nanocomposites: A review. Prog Polym Sci 2011;36: 914-944.
[23] Campilho RDSG, de Moura MFSF, Pinto AMG, Morais JJL, Domingues JJMS. Modelling the tensile fracture behaviour of CFRP scarf repairs. Compos Part B–Eng 2009;40:149–157
[24] Khashaba, U.A., Othman, R. Low-velocity impact of woven CFRE composites under different temperature levels. International Journal of Impact Engineering 2017;108:191-204.
[25] Gkikas G, Sioulas D, Lekatou A, Barkoula NM, Paipetis AS. Enhanced bonded aircraft repair using nano-modified adhesives. Materials and Design 2012;41:394-402.
[26] Priem C, Othman R, Rozycki P, Guillon D. Experimental investigation of the crash energy absorption of 2.5D-braided thermoplastic composite tubes. Compos Struct 116 (2014) 814-826.
[27] Khashaba UA. Improvement of toughness and shear properties of multi-walled carbon nanotubes/epoxy composites. Polymer composites 39(2017)815-825.

[28] David-West OS, Nash DH, Banks WM. Low-velocity heavy mass impact response of singly curved composites. Proceedings of the Institution of Mechanical Engineers, Part L: Journal of Materials: Design and Applications 228 (2014) 17-33.
[29] Alnefaie KA, Aldousari SA, Khashaba UA. New development of self-damping MWCNT composites. Composites: Part A 52 (2013) 1-11.
[30] Baldan A. Adhesion phenomena in bonded joints. Int J Adhes Adhes 2012;38:95–116.
[31] Falvo MR, Taylor II RM, Helser A, Chi V, Brooks Jr FP, et al. Nanometre-scale rolling and sliding of carbon nanotubes. Nature 1999;397:236-7.
[32] Khan SU, Li CY, Siddiqui NA, Kim J-K. Vibration damping characteristics of carbon fiber-reinforced composites containing multi-walled carbon nanotubes. Compos Sci Technol 2011;71:1486-94.
[33] Karapappas P, Vavouliotis A, Tsotra P, Kostopoulos V. Enhanced Fracture Properties of Carbon Reinforced Composites by the Addition of Multi-Wall Carbon Nanotubes. J Composite Materials 2009;43:977–985.
[34] Quan D, Urdániz JL, Ivanković A. Enhancing mode-I and mode-II fracture toughness of epoxy and carbon fibre reinforced epoxy composites using multi-walled carbon nanotubes. Materials and Design 2018;143: 81–92
[35] El-Qoubaa Z, Othman R. Strain rate sensitivity of polyetheretherketones' compressive yield stress at low and high temperature. Mech Mater 2016 ;95 :15-27.
[36] Agarwal A, Foster SJ, Hamed E. Testing of new adhesive and CFRP laminate for steel-CFRP joints under sustained loading and temperature cycles. Compos Part B Eng 2016;99: 235-247.
[37] Challita G, Othman R, Khalil K. Compression and shear behavior of epoxy SA 80 bulk adhesive over wide ranges of strain rate. J Polym Eng 2016;36:165-171.
[38] El-Qoubaa Z, Othman R. Characterization and modeling of the strain rate sensitivity of polyetheretherketone's compressive yield stress. Materials and Design 2015;66:336-345.